Research on Enhancing Speed Measurement Accuracy in Rail Transit Systems Using Curve Fitting Techniques

Yimin Li(✉)

China Airport Construction Group Corporation, Beijing 100010, China
xz2646@sina.com

Abstract. Urban rail systems depend on speed sensors for velocity measurements, which often face challenges such as noise interference and sampling delay errors, particularly at low speeds. This study delves into the hardware structure, measurement principles, speed calculation methods, and the root causes and impacts of sampling errors on train control. A novel approach employing least squares curve fitting is proposed to tackle these issues. Our research endeavors to augment the efficacy and safety of urban rail systems by augmenting low-speed speed detection's precision and dependability. To authenticate the efficacy of the suggested technique, we conducted rigorous simulation tests. The study's results unveil auspicious strides in fortifying the security and steadfastness of rail operations, thereby accentuating the latent potential harbored within the proposed method to optimize urban rail systems.

Keywords: Electrical equipment · Speed detection technology · Speed sensor

1 Introduction

Urban rail systems are a fundamental infrastructure, providing convenient and accurate transportation for citizens. Urban rail transit systems bestow upon residents an exalted quality of life, as they deftly optimize the flow of urban traffic. However, maintaining the stable operation and safety of urban rail transit requires a deep understanding and research of many key technologies, among which speed detection technology is particularly critical [1, 2].

Speed detection plays a crucial role in the operation of urban rail trains, directly affecting several important aspects such as train operating speed, braking efficiency, and driving stability. Especially during the braking process of asynchronous motors, precise speed detection is necessary. In the realm of speed detection, the prevailing methodologies encompass the utilization of velocity gauges for the purpose of speed quantification, as well as discernments devoid of such velocity gauges.

The speed observation method doesn't rely on hardware devices like speed sensors and offers advantages such as cost-effectiveness, compact size, and easy maintenance. While theoretically, this method can achieve higher precision by directly measuring

M. Gong et al. (Eds.): EITRT 2023, LNEE 1138, pp. 28–36, 2024.
https://doi.org/10.1007/978-981-99-9319-2_4

motor parameters, its accuracy can be affected by factors like data errors and motor model parameter variations. Hence, in practical applications, it may not attain the same level of precision as speed measurement using speed sensors [3].

The primary merits inherent in the method of speed measurement employing velocity sensors reside within its lofty precision and unwavering constancy. By directly ascertaining the velocity of objects, its measurement outcomes typically manifest heightened accuracy, thereby adeptly mirroring the veritable circumstances at hand. This speed measurement method has been widely used in commercial products.

2 Principle of Speed Sensor

2.1 Hardware Model Analysis of Speed Sensor

Figure 1 displays an internal gear structure of the speed sensor of the urban rail train control system, which furnishes speed signals [4]. For simple applications, a single output signal and one track on the encoder disk are sufficient to meet the requirements. However, for more complex applications with stricter safety requirements, multiple output signals or two tracks on the encoder disk are needed. To deduce the trajectory of locomotion, the disparity in phase betwixt the pair of emitted signals is harnessed, serving as a determinant of travel direction.

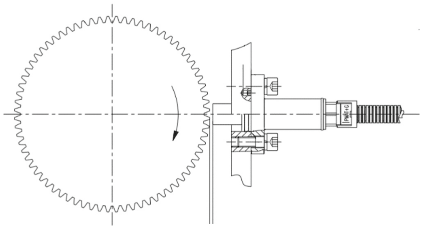

Fig. 1. Speed sensor mechanical interface

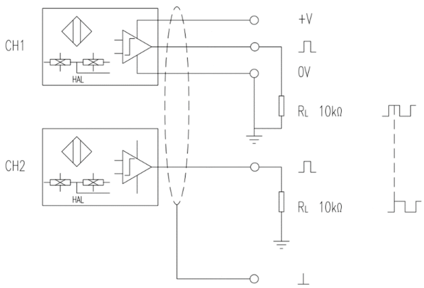

Fig. 2. Output waveform of the speed sensor

The speed sensor used on urban rail trains is an incremental optical speed sensor. A device dedicated to detecting rotational angular displacement manifests assemblage, relinquishing dual square wave pulse signals emanating from an axle's revolution.

These signals, elegantly depicted in Fig. 2 [5], when subjected to meticulous scrutiny of their phase correlation, endow the capability to discern the motor's rotational direction. Henceforth, this discernment unveils insights into the motion state of the train during that particular temporal juncture.

2.2 The Theory of Speed Measurement

To fathom the realm of velocity assessment leveraging the pulse waveform output harnessed from the speed sensor, a duo of distinct methodologies has been scrupulously forged: The M-method and the T-method. The following analysis will focus on these two methods [6].

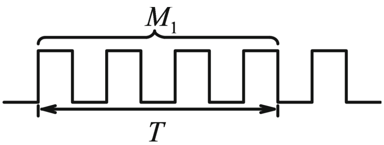

Fig. 3. M-method

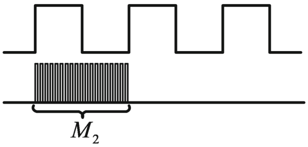

Fig. 4. T-method

As vividly depicted in Fig. 3, the underlying principle governing the M-method of speed measurement resides in the meticulous enumeration of the quantum of pulses M_1, gratuitously dispensed by the speed sensor, spanning a steadfast temporal interval T. The speed within T is deduced by computing the rotational angle in a single unit of time. Using the M-method:

$$n = \frac{60N_M}{N_p T} \tag{1}$$

During instances of diminished velocity, the allotted temporal span for measurement becomes truncated, thus engendering a diminished tally when employing the M-method. Consequently, this decrement in count imparts a more substantial influence of error. However, as the train speed increases, the time between pulses decreases, leading to an increased count and improved accuracy with the M-method, as shown in Fig. 4. Using the T-method:

$$n = \frac{60f_T}{N_p M_2} \tag{2}$$

At elevated speeds, the T-method detects a paucity of pulses; however, as the rotational velocity diminishes, the discerned pulse count experiences a gradual augmentation. The T-method's accuracy in speed measurement is enhanced as a consequence.

3 Causes of Speed Measurement Errors

The origins of errors in speed sensors predominantly encompass hardware-induced discrepancies and theoretical inconsistencies, both of which bear substantial influence on the resultant measurement outcomes [7]. This section will primarily focus on the study of theoretical errors.

3.1 Theoretical Errors in Speed Sensor Speed Measurement Sampling

Speed sensors behave like zero-order hold in analog-to-digital conversions. They convert pulse signals into discrete step signals, introducing delay errors that are more prominent at low speeds.

Speed measurement results are digital signals that represent time intervals between periods [8]. Adjusting measurement standards, such as detecting both rising and falling edges of sensor pulses, can improve speed measurement, especially for sensors with low resolution [9]. However, achieving accurate orthogonal relationships and uniform pulse distribution with a 50% duty cycle is challenging in real-world applications.

Regardless of the speed measurement method, there will always be a certain delay in the sampled output. This delay causes slight underestimations during acceleration and slight overestimations during deceleration, particularly noticeable at low speeds.

3.2 The Impact of Sampling Errors on Control Systems

Speed measurement in indirect vector control of asynchronous motors is influenced by various factors such as speed PI controller parameters, speed sampling frequency, speed itself, and the torque command value. Larger sampling times result in greater angular errors and introduce inaccuracies in torque control, especially at speeds below 5 km/h.

By scrutinizing the ramifications of speed sampling errors on velocity control, it is plausible to simplify the current loop as an elementary inertia element of first-order. Increased sampling times lead to greater phase lag and smaller phase stability margins, affecting system responses under the same PI parameters. When the speed sensor sampling frequency is sufficiently high, the current loop can achieve minimal overshoot and phase lag, resulting in better performance. However, insufficient sampling frequency leads to limitations in the current loop's bandwidth, affecting the speed control system due to significant peak resonance value and phase lag [10].

4 Reducing Speed Measurement Errors Through Curve Fitting

Minimizing disparities between the fitted curve and the data points is the goal of curve fitting, with a focus on minimizing deviations rather than accurately navigating each point [11]. The goal is to ensure that all points closely align with the curve, effectively reducing local fluctuations. In the case of continuous and high-inertia systems such as urban rail trains, the least squares curve fitting method is suitable for estimating the train's running speed and motor speed.

4.1 Least Squares Principle

In a certain function class ϕ:

$$\phi = \{\phi_0(x), \phi_1(x), \cdots \phi_n(x)\} \tag{3}$$

There exists a function $\phi(x)$ such that:

$$\varphi^*(x) = a_0^*\varphi_0(x) + a_1^*\varphi_1(x) + \cdots + a_n^*\varphi_n(x) \tag{4}$$

Satisfying the condition:

$$\sum_{i=1}^{m} [\varphi * (x_i) - y_i]^2 = \min_{\varphi(x)\in\Phi} \sum_{i=1}^{m} [\varphi(x_i) - y_i]^2 \tag{5}$$

where:

$$\varphi(x) = a_0\varphi_0(x) + a_1\varphi_1(x) + \cdots + a_n\varphi_n(x) \tag{6}$$

can be any function in the function class ϕ.

Taking the function $\varphi_i(x)$ as:

$$\varphi_i(x) = x^i \tag{7}$$

We obtain the algebraic polynomial:

$$\begin{cases} \varphi(x) = a_0 + a_1x + a_2x^2 + \cdots + a_nx^n \\ (\varphi_k, f) = \sum_{i=1}^{N} x_i^k y_i (k = 0, 1, \cdots, m) \end{cases} \tag{8}$$

By performing a matrix transformation to:

$$\begin{bmatrix} \sum_{i=1}^m 1 & \sum_{i=1}^m x_i & \cdots & \sum_{i=1}^m x_i^n \\ \sum_{i=1}^m x_i & \sum_{i=1}^m x_i^2 & \cdots & \sum_{i=1}^m x_i^{n+1} \\ \vdots & \vdots & & \vdots \\ \sum_{i=1}^m x_i^n & \sum_{i=1}^m x_i^{n+1} & \cdots & \sum_{i=1}^m x_i^{2n} \end{bmatrix} \begin{bmatrix} \alpha_0 \\ \alpha_1 \\ \vdots \\ \alpha_n \end{bmatrix} = \begin{bmatrix} \sum_{i=1}^m y_i \\ \sum_{i=1}^m x_iy_i \\ \vdots \\ \sum_{i=1}^m x_i^ny_i \end{bmatrix} \tag{9}$$

Urban rail trains typically have weights in the hundreds of tons, and their systems have high inertia. Therefore, the vehicle speed does not undergo abrupt changes during operation, and the traction motor speed can be considered as a continuous variation. Whose elements are typically represented as:

$$\varphi(x) = a_0 + a_1x + a_2x^2 + \cdots + a_nx^n \tag{10}$$

Whilst engrossed in the fitting process, let us posit the order of the fitting function to be n. It becomes necessary to establish the extent of the sampling interval, denoted as N, and identify the precise time point, represented by N′, for prediction calculations. We collect m measurement values from the speed sensor as the initial conditions for the calculation. Let's denote the corresponding reference speeds for the N points as $n_1, n_2, \cdots n_N$ and assign a unique index $1, 2, \cdots N$ to each sample.

At the current time t:

$$n_N = n_{\mathrm{t}} \tag{11}$$

When a new velocity measurement value n_{t+1} is obtained at the next time $t+1$, the first sampled value with the initial index is discarded. The remaining data points are shifted forward in terms of their corresponding indices, updating the values of $n'_1, n'_2, \cdots n'_N$ and their corresponding indices $1, 2, \cdots N$. Using the least squares method for velocity fitting, the novel coefficients are computed, thus avoiding any alteration to the sampling interval's initial length, thus preserving consistency. The process can be represented by the following equation:

$$\begin{cases} n'_{N-1} = n_N \\ n'_N = n_{t+1} \end{cases} \quad n = 1, 2, \cdots, N \tag{12}$$

Considering the large inertia of urban rail trains and the fact that the deceleration and braking process can be modeled as a first-order function, high-order polynomial curve fitting can easily lead to ill-conditioned problems.

5 Simulation Verification

Integrating the angle of rotation in a unit of time can generate the corresponding pulse signals. In practical engineering, a speed sensor with 60 teeth is commonly used for speed measurement. Therefore, for simulation purposes, we will use a model of a 60-tooth speed sensor. The parameters for simulation experiment are presented in Table 1.

Table 1. The simulation experiment parameters

Parameter	Value
Simulation step size	$2e^{-6}$
Interrupt frequency of the DSP	1k
Number of teeth on the speed measuring gear	60
Method	T-method
White-noise	10%
Order for the fitting function	1
Sampling interval values for the fitting function	200
Calculation points for the fitting function	15

5.1 Speed Measurement Error Correction

After the speed signal, which encompasses noise, is sampled by the speed sensor, it proceeds through a series of processing steps entailing the utilization of the least squares fitting algorithm. To emulate the repercussions of veritable speed sensor sampling errors, a viable approach involves integrating an error component into the simulated speed signal. This is achieved by infusing 10% white noise into the speed signal, thereby engendering a composite signal that faithfully emulates the sampling errors encountered during real-world operations. The resultant amalgamated signal exhibits instability and substantial fluctuations, as exemplified in Fig. 5.

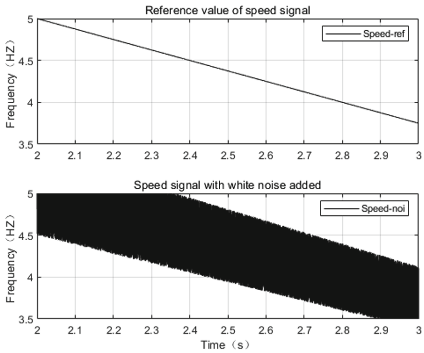

Fig. 5. Speed signal with white noise added

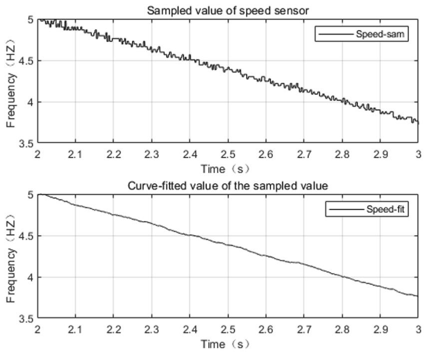

Fig. 6. Curve-fitted valve of the simple value

Following the sampling of the speed signal containing noise by the speed sensor, it undergoes processing employing the least squares fitting algorithm. The outcome is a meticulously fitted speed curve that closely aligns with the ideal signal. Through this fitting process, fluctuations within the speed measurement curve are mitigated, resulting in a reduction of errors, as exemplified in Fig. 6.

5.2 Sampling Delay Correction

Table 1 showcases the parameter values germane to the simulation experiment, constituting the pivotal elements subject to adjustment in the realm of least squares curve fitting. These parameters encompass the fitting function's order, the temporal span of the sampling interval, and the designated points utilized for prediction calculations.

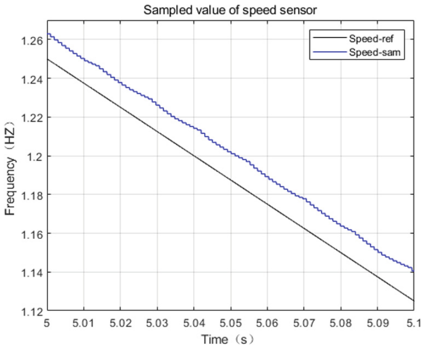

Fig. 7. Sample value of speed sensor

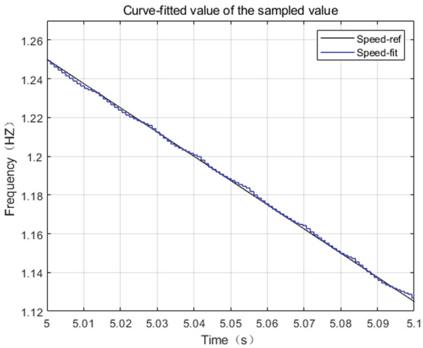

Fig. 8. Curve-fitted valve of the simple value

The speed sensor exhibits a certain delay in measuring velocity, which is more pronounced at low speeds due to the nature of the digital DSP control system, as shown in Fig. 7. Analyzing the simulation waveform reveals that a larger prediction calculation point results in a more significant advancement effect on the fitted velocity value. A suitable calculation point should be chosen during the control process, considering the actual conditions and the inherent delay error of the system, as shown in Fig. 8.

6 Conclusion

This article meticulously examines the mechanical structure and speed measurement principles governing the speed sensor. It delves into the implementation techniques of control system software, expounds on speed measurement methodologies, elucidates the origins of speed measurement errors, and assesses their consequential impact on control precision. Specifically, it scrutinizes system errors and delay errors inherent in speed measurement during low-speed conditions and proposes a novel approach employing the least squares curve fitting technique. Through comprehensive simulations, the article verifies the efficacy of curve fitting, thus effectively enhancing the accuracy of speed detection for urban rail transit trains operating in low-speed scenarios.

References

1. Yun, C.M., Cho, G., Kim, H., et al.: A study on the train brake position-based control method for regenerative inverters [J]. Energies **15** (2022). https://doi.org/10.3390/en15186572
2. Pagliara, F., Papa, E.: Urban rail systems investments: an analysis of the impacts on property values and residents' location[J]. J. Transp. Geogr. **19**(2), 200–211 (2011). https://doi.org/10.1016/j.jtrangeo.2010.02.006
3. Yin, J., Ren, X., Liu, R., et al.: Quantitative analysis for resilience-based urban rail systems: a hybrid knowledge-based and data-driven approach[J]. Reliab. Eng. Syst. Saf. **219**, 108183 (2022). https://doi.org/10.1016/j.ress.2021.108183
4. Zhiwen, L., Qin, Y., Wang, M.: Research on high-speed railway operation adjustment model based on priority. Smart Resilient Transp. **4**(1), 12–21 (2022). https://doi.org/10.1108/SRT-04-2021-0005
5. Mahmoodi, A., Jasemi Zergani, M., Hashemi, L., Millar, R.: Analysis of optimized response time in a new disaster management model by applying metaheuristic and exact methods. Smart Resilient Transp. **4**(1), 22–42 (2022). https://doi.org/10.1108/SRT-01-2021-0002
6. Zhao, C., Dong, X., Dong, K.: Quantifying the energy trilemma in China and assessing its nexus with smart transportation. Smart Resilient Transp. **4**(2), 78–104 (2022). https://doi.org/10.1108/SRT-05-2022-0008
7. Zuloaga, S., Vittal, V.: Metrics for use in quantifying power system resilience with water-energy nexus considerations: mathematical formulation and case study [C]. IEEE Power Energy Soc. Gen. Meet. (PESGM). IEEE (2019). https://doi.org/10.1109/PESGM40551.2019.8973943
8. Al-Mutayeb, Y., Almobaied, M.: Luenberger observer-based speed sensor fault detection of BLDC motors [C]. In: International Conference on Electric Power Engineering – Palestine (ICEPE- P) (2021). https://doi.org/10.1109/ICEPE-P51568.2021.9423483
9. Wu, Q., Li, G., Qi, X., et al.: Research on the low speed performance of speed sensor-less vector control system[C]. In: 2015 IEEE 10th conference on industrial electronics and applications (ICIEA). IEEE (2015). https://doi.org/10.1109/ICIEA.2015.7334336
10. Zhang, M., Han, J.: Analysis and compensation of disturbance for small inertial stabilized Line-of-Sight system[C]. In: Society of Photo-optical Instrumentation Engineers. Society of Photo-Optical Instrumentation Engineers (SPIE) Conference Series (2017). https://doi.org/10.1117/12.2257355
11. Chang, L., He, T., Wang, C., et al.: Multi-surface phase-shifting interferometry using harmonic frequency solution based on the total least squares [J]. Opt. Lasers Eng. 150 (2022). https://doi.org/10.1016/j.optlaseng.2021.106845